Dynamic modeling and linear model predictive control of gas pipeline networks

Guang-Yan Zhu [a], Michael A. Henson [a,*], Lawrence Megan [b]

[a]*Department of Chemical Engineering, Louisiana State University, Baton Rouge, LA 70803-7303 USA*
[b]*Process and Systems, Research and Development, Praxair, Inc., Tonawanda, NY 14151-0044, USA*

Abstract

A linear model predictive control (LMPC) strategy is developed for large-scale gas pipeline networks. A nonlinear dynamic model of a representative pipeline is derived from mass balances and the Virial equation of state. Because the full-order model is ill-conditioned, reduced-order models are constructed using time-scale decomposition arguments. The first reduced-order model is used to represent the plant in closed-loop simulations. The dimension of this model is reduced further to obtain the linear model used for LMPC design. The LMPC controller is formulated to regulate certain pipeline pressures by manipulating production set-points of cryogenic air separation plants. Both input and output variables are subject to operational constraints. Three methods for handling output constraint infeasibilities are investigated. © 2001 Elsevier Science Ltd. All rights reserved.

Keywords: Gas pipelines; Model predictive control; Constraints

1. Introduction

The chemical and steel industries consume large quantities of purified nitrogen and oxygen. In regions highly concentrated with these industries, purified gases are produced by cryogenic air separation plants and supplied via extensive pipeline networks. The oxygen pipeline network considered in this paper is representation of those operated by Praxair. The pipeline is over 50 miles long and has approximately 15 customers. Pipeline pressures must be maintained near their desired values without violating constraints imposed by safety concerns and business contracts. The desired pressures may correspond to a certain economic optimum, such as the low pressure limits at all customer sites. When the pipeline pressure drops below the lower limit, vaporized liquid oxygen must be introduced to the pipeline to quickly increase the pressure. Emergency vents must be opened to release gas when the pressure exceeds the upper limit. Both situations result in economic penalties and should be prevented.

Heuristic operating guidelines for long distance natural gas transmission pipeline scan be found in [7]. These pipelines have much longer pipes and simpler configurations than the oxygen pipeline studied here. A partial differential equation (PDE) model of a natural gas pipeline is proposed by Guy [11]. Finite difference solution of this model is investigated by Lappus and Schmidt [12]. Commercial software packages for dynamic gas pipeline simulation include WinTran by Gregg Engineering [4] and PIPESYS by Hyprotech [5]. Based on the dynamic simulator GANESI [19], Marques and Morari [13] develop an optimization strategy based on quadratic programming to reduce compressor costs of natural gas pipelines. The literature on gas pipeline control is rather sparse. Sanada and Kitagawa [18] formulate a linear H_∞ controller for a very simple gas pipeline described by ordinary differential equations that are obtained by discretizing a PDE model. Several articles [3,8] suggest that the natural gas industry relies on simple regulatory control strategies and uses pipeline models primarily for early fault detection.

Current industal practice for oxygen/nitrogen pipeline control involves regulatory control loops along with manual intervention by pipeline operators. Regulatory control loops are used to maintain certain pipeline pressures and flows. However, pipeline pressures are

---

* Corresponding author. Tel.: +1-225-388-3690; fax: +1-225-388-1476.

E-mail address: henson@che.lsu.edu (M.A. Henson).

determined ultimately by the production rates of the cryogenic plants supplying the pipeline. Operators determine the production setpoint of each air separation plant manually by analyzing the current customer demands and pipeline pressures. This current practice is inadequate for achieving optimal operation of the pipeline. With the implementation of linear model predictive control (LMPC) on individual cryogenic plants, it is now possible to achieve closed-loop control of the pipeline network by using the plant production rate setpoints as manipulated inputs. The pipeline LMPC controller proposed in this paper is designed to drive critical pressures to setpoints determined by the operations staff or a higher level steady-state optimizer. Important cryogenic plant constraints can be included explicitly when the pipeline controller computes the plant production setpoints.

LMPC has been widely accepted by the chemical industry due to its multivariable formulation and constraint handling abilities. The pipeline control problem is a good candidate for LMPC because it is a highly interacting and highly constrained process. A related application of LMPC to a combined sewer system is studied by Gelormino and Ricker [10]. According to their paper, implementation of LMPC has achieved significant reduction of combined sewer overflows, which is a critical case of constraint violation. A comprehensive review of industrial LMPC technology can be found in [16]. The LMPC controller utilized in this paper is the infinite horizon formulation proposed by Muske and Rawlings [15]. This formulation ensures nominal stability for stable and unstable systems subject to both input and output constraints [14,17]. Output constraint infeasibilities are handled by completely removing the output constraints over a portion of the prediction horizon. The stability of infinite horizon LMPC with a soft output constraint handling method is examined by Zheng and Morari [24]. Both output constraint handling techniques are studied in [20] and in this paper.

The remainder of the paper is organized as follows. In Section 2, dynamic modeling of a representative oxygen pipeline network is discussed and open-loop simulation results are presented. Formulation of the LMPC problem for the oxygen pipeline is described in Section 3. Section 4 contains closed-loop simulation results for the oxygen pipeline example. Finally, a summary and conclusions are given in Section 5.

2. Dynamic modeling of gas pipeline networks

Fig. 1 is a schematic of the oxygen pipeline considered in this paper. Each number indicates a production site, a customer site or a pipe junction. They are called "nodes" in the sequel. The control valve that divides the high pressure and low pressure sides of the pipeline is known as the "let-down station". The let-down station offers an additional manipulated variable that is especially effective for controlling the low pressure side of the
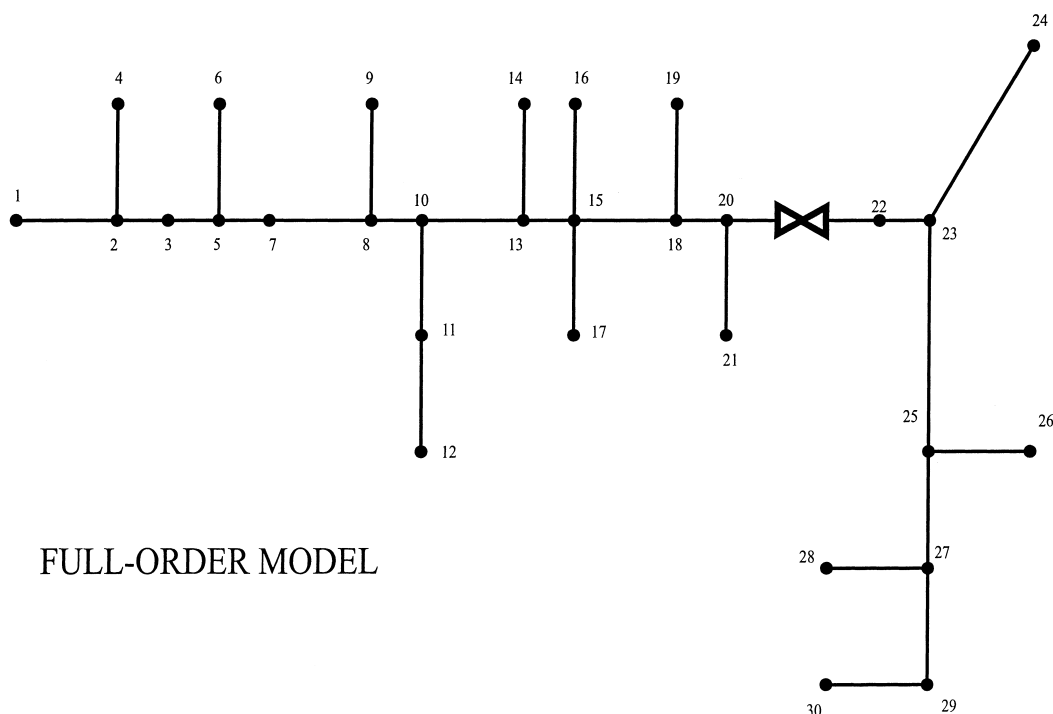

Fig. 1. Full-order pipeline network (30 nodes).

pipeline. The let-down station also is important for extreme conditions such as a plant shutdown on the high pressure side of the pipeline. When this occurs, the let-down station valve can be closed to maintain pressure on the high pressure side.

A first-principles model is derived to describe the pressure dynamics of the oxygen pipeline. We are primarily interested in pressure changes at each node rather than a detailed description of the spatial pressure gradients. While a PDE model offers accurate description of the gas transmission dynamics and is suitable for infrequent on-line optimization, it is unnecessarily complex for model-based control at the frequency of minutes. Therefore we construct an ordinary differential equation (ODE) model that only describes the pressure changes at the nodes. Although not discussed here for proprietary reasons, the proposed model compares favorably with Praxair's internal dynamic model derived from plant tests.

The complete pipeline model is composed of three groups of equations: (i) node pressure equations; (ii) let-down station pressure control loop equations; and (iii) cryogenic plant production and constraint variable equations. The second set of equations describe the pressure control loop for the let-down station. The third set of equations represent the closed-loop cryogenic plant production dynamics and dynamic relations between other plant constraint variables and the production rates. Approximate closed-loop dynamics of the LMPC controlled cryogenic plants are included to eliminate the need for detailed modeling.

2.1. Full-order nonlinear model

Node pressure equations are derived from molar balances at each node. Energy balances are not needed because the temperature changes in the pipeline are negligible. The molar balance for node i is:

$$\dot{N}_i = \rho_{sc}\left[\sum_k F_{i,k} + \sum_j f_1(P_i, P_j, \theta)\right] \tag{1}$$

where N_i is the gas molar holdup at node i, ρ_{sc} is the molar density of oxygen at standard conditions (1 atm and 60°F), $F_{i,k}$ is the volumetric gas flow rate from a production plant (positive flow) or to a customer (negative flow) at node i. A complete set of nomenclature is shown in Appendix A. The subscript k denotes the production plant k at nodes $i = 10, 24$, and 29; $k = 1$ for customer withdraws at all other nodes. The function $f_1(P_i, P_j, \theta)$ represents the volumetric flow rate between node i and node j. The flow depends on the associated pressures (P_i and P_j) and the pipeline leg parameters (θ). A leg connects two nodes and can be a pipe or a valve.

For a pipe f_1 takes the form of the Weymouth equation [1], which can be derived from a momentum balance and is used extensively in the gas industry for modeling compressible flows:

$$f_1(P_i, P_j) = 114.2\sqrt{\frac{\left(P_i^2 - P_j^2\right)d_p^5}{f_r L T S_g}\frac{E_f}{Z_m}} \tag{2}$$

where d_p is the pipe diameter, f_r is the friction factor, L is the pipe length, T is the temperature, S_g is the specific gravity of the gas, E_f is the efficiency factor and Z_m is the mean compressibility of the gas. The friction factor (f_r) is estimated using the formula [1]:

$$f_r = \frac{0.032}{d_p^{1/3}}$$

The efficiency factor (E_f) is assumed to be one. For the let-down station, linear valve dynamics are assumed and the flow equation is:

$$f_1(P_i, P_j, l) = C_v\frac{l}{100}\sqrt{\frac{P_i - P_j}{S_g}} \tag{3}$$

where l is the percentage of valve opening and C_v is the valve characteristic constant. This equation is appropriate because the let-down station pressure does not change significantly from the nominal value and the pressure drop across the valve is only around 10% of P_i.

Since the molar holdup at each node cannot be measured, it is desirable to have the node pressures as dependent variables in the model equations. This is achieved by assuming each node has a constant volume. The node volumes are determined by dividing the pipe volumes equally among the adjacent nodes. Each node molar volume is related to its associated node pressure by an equation of state. Commonly used cubic equations of state (e.g. [23]) yield very complicated expressions for the pressure derivatives. For the pressure range of a typical oxygen pipeline, the Virial equation of state [23] provides good prediction of gas properties and makes the resulting model much simpler. Using the truncated Virial equation, the molar holdup at node i can be expressed as:

$$N_i = \frac{V_i P_i}{Z_i R T} = \frac{V_i P_i}{R T + B_i P_i} \tag{4}$$

where R is the gas constant, B_i is the second Virial coefficient for node i and V_i is the node volume. Taking time derivatives on both sides of (4) yields:

$$\frac{dN_i}{dt} = \frac{V_i R T}{(R T + B_i P_i)^2}\frac{dP_i}{dt} \tag{5}$$

Substituting (5) into the node molar balance Eq. (1) yields:

$$\frac{dP_i}{dt} = \rho_{sc}f_2(P_i)\left[\sum_j f_1(P_i, P_j) + \sum_k F_{ik}\right] \quad (6)$$

where the function f_2 is defined as:

$$f_2(P_i) = \frac{(RT + B_iP_i)^2}{V_iRT}$$

The let-down station pressure control loop is described by following equations:

$$l = l_{ss} + K_c e_f + \frac{K_c}{\tau_I}\eta_f \quad (7)$$

$$\dot{\eta} = P_{sp} - P \quad (8)$$

$$\dot{e}_f = \frac{1}{\tau_f}\left[(P_{sp} - P) - e_f\right] \quad (9)$$

$$\dot{\eta}_f = \frac{1}{\tau_f}(\eta - \eta_f) \quad (10)$$

where l and l_{ss} are the valve position and steady-state valve position, respectively; K_c and τ_I are tuning parameters for the PI regulator; e_f is a filtered value of the difference between the pressure (P) and its setpoint (P_{sp}); η is the integrated error; and η_f is the filtered value of η. The error signals are filtered to reduce large valve movements which can cause numerical problems when the full-order model is simulated. The pressure control loop equations are included explicitly in the model because the LMPC controller manipulates the let-down pressure setpoint (P_{sp}).

The production rates (F_i) of the LMPC controlled cryogenic plants are modeled empirically as first-order-plus-deadtime (FOPDT) systems:

$$\frac{dF_i}{dt} = \frac{1}{\tau_i}[Frq_i(t - t_d) - F_i(t)] \quad (11)$$

where τ_i is the closed-loop time constant for the ith production plant and Frq_i is the production request (setpoint). All the cryogenic plant models have the same deadtime t_d. The FOPDT model parameters are obtained from closed-loop plant data. The dynamics of the other constraint variables ($\Gamma \epsilon R^{10}$) associated with individual cryogenic plants are described by a set of ordinary differential equations and algebraic equations derived from the empirical relations (11). These constraint variables includes air flow rates, liquid nitrogen production rates, total compressor flow rates and power consumptions. These plant constraints must be honored

because of equipment limits and business contracts. The associated equations are not shown in this paper for proprietary reasons. While the plant constraints are included in the subsequent simulations, it should be noted that the constraints are not active during any of the simulation tests. Thus, identical results will be obtained if the plant constraints are omitted. A complete set of model equations excluding the plant constraint variables is included in Appendix B.

2.2. Reduced-order nonlinear models

The full-order model of the oxygen pipeline is comprised of 43 ordinary differential equations and seven algebraic equations. Thirty differential equations describe the node pressure changes along the pipeline. The node pressure dynamics are determined primarily by the physical dimensions of the adjacent legs. Due to large differences in leg lengths (50–161,200 ft), the full-order model exhibits multiple time scales. As discussed below, the pipeline network is an integrating system and therefore the linearized system matrix A has a zero singular value. The large difference in time scales is exemplified by the very wide range of nonzero singular values (0.1705–3.083×10^7). As a result, numerical problems are encountered when the full-order model is used as the basis for LMPC design.

One approach for improving the conditioning of the model is to combine adjacent nodes with small pressure drops. This eliminates short pipes with fast dynamics and also reduces the total number of model equations. To construct reduced-order pipeline models, the following guidelines are followed:

1. The new pipe lengths are the sum of the combined pipe lengths.
2. The new pipe diameters are determined such that the total volume of the combined legs is preserved.
3. The pipe efficiency factors are adjusted such that the difference between the steady-state solutions of the full-order and reduced-order models are minimized in a least-squares sense.
4. The volumes corresponding to eliminated nodes are distributed between adjacent nodes to achieve more uniform time scales.

The full-order pipeline model first is reduced from 30 nodes to 19 nodes by eliminating short lateral legs. As shown later, there is very little difference between the reduced-order and full-order model predictions. But the reduced-order model is better conditioned as shown by the range of non-zero singular values (0.1884–4.168×10^5). This reduced-order model serves as the plant in closed-loop simulations. The model is reduced further to only 10 nodes to generate the model used for LMPC design. This reduction is performed such that

the node pressures subsequently defined as controlled outputs remain explicitly in the model. The non-zero singular value range (0.0987–5.1401×10^4) shows that the controller model is slightly better conditioned than the plant model. Figs. 1–3 show the pipeline layouts corresponding to the three models. Table 1 show the definition of the reduced-order model nodes in terms of the full-order model nodes.

2.3. Linear controller design model

The linear model used for LMPC design is obtained by linearizing the nonlinear controller model at a steady-state operating point. The pipeline network is an integrating system because it contains an inventory of gas. Consequently, for any set of inputs there exists an equilibrium space rather than isolated equilibrium
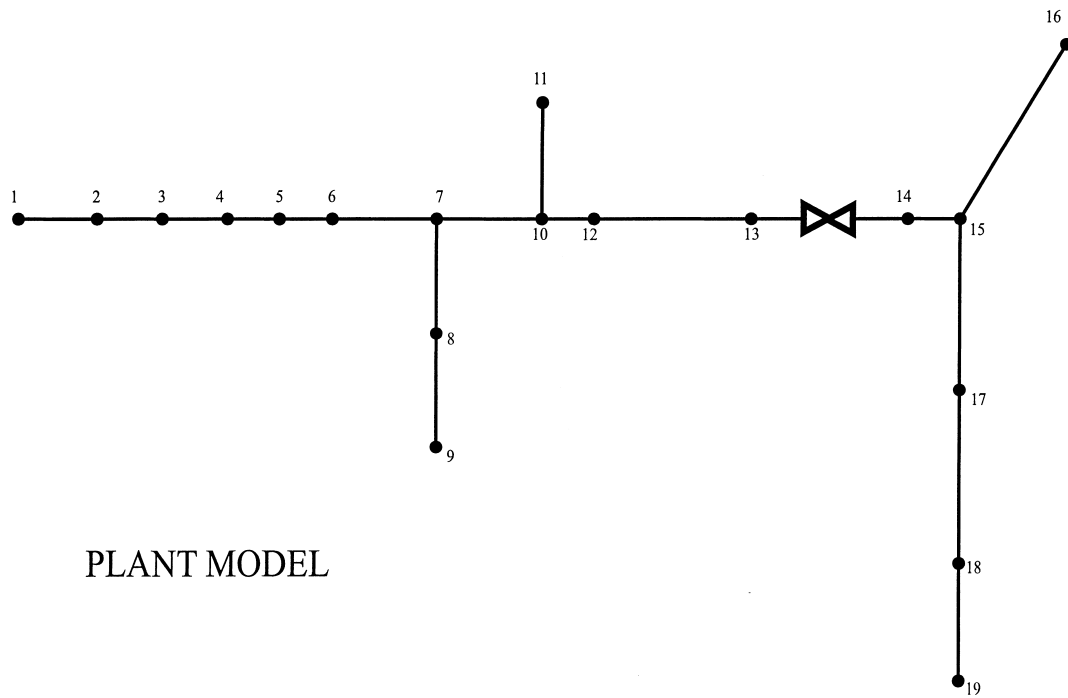
Fig. 2. Reduced-order pipeline network for the plant model (19 nodes).
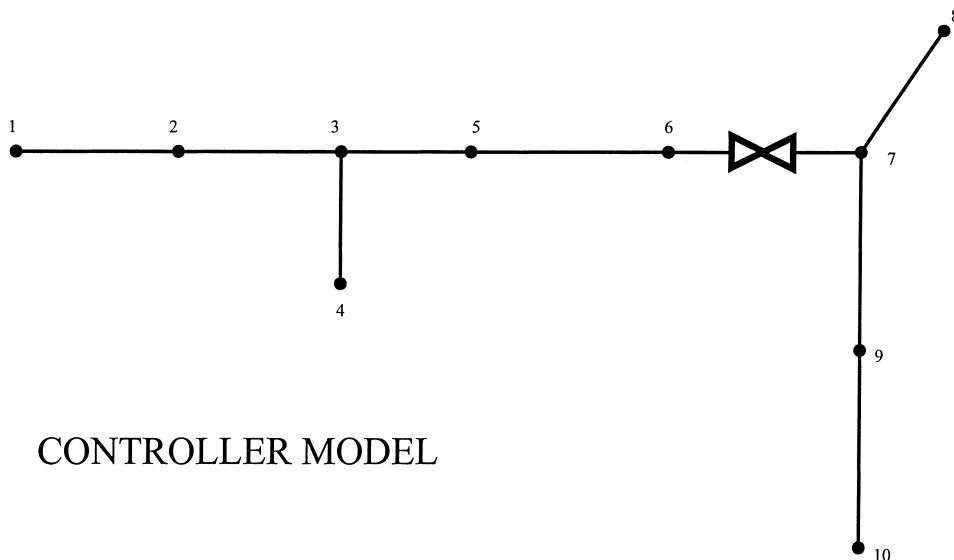
Fig. 3. Reduced-order pipeline network for the controller model (10 nodes).

points. The steady-state values used for linearization correspond to the nominal operating condition for the pipeline. The resulting linear controller design model has the form:

$$x(k+1) = Ax(k) + Bu(k) + B_{\mathrm{d}}d(k)$$

$$y(k) = Cx(k)$$

$$y_c(k) = C_c x(k) + D_{\mathrm{d}}d(k) \qquad (12)$$

where $x \in R^{23}$ is the vector of state variables shown in Table 1, $u \in R^6$ is a vector of manipulated inputs, $d \in R^{10}$ is a vector of measured disturbances, $y \in R^3$ is a vector of controlled outputs, $y_c \in R^{14}$ is a vector of constrained outputs and k is the discrete time index. The sampling time is 2 min.

The state vector consists of the node pressures, the cryogenic plant production rates, the let-down station control loop variables, and plant constraint variables:

$$x = \Big[P_{1-4} \; P_{5-9} \; P_{10} \; P_{11,12} \; P_{13-17} \; P_{18-21} \; P_{22,23}$$

$$P_{24} \; P_{25,26} \; P_{27-30} \; F_{10,2} \; F_{10,3} \; F_{24,1}$$

$$F_{24,2} \; F_{29,1} \; \eta \; e_{\mathrm{f}} \; \eta_{\mathrm{f}} \; \Gamma_x^T \Big]^T \qquad (13)$$

where the subscripted P terms denote node pressures for the controller model based on Fig. 3 and $\Gamma_x \in R^5$ is the subset of plant constraint variables contained in the state vector. The input vector is comprised of the pro-

duction requests for the five LMPC controlled cryogenic plants and the pressure setpoint for the let-down station:

$$u = \Big[Frq_{10,2} \; Frq_{10,3} \; Frq_{24,1} \; Frq_{24,2} \; Frq_{29,1} \; P_{\mathrm{sp}} \Big]^T$$

It is assumed that the production requests are delayed by one sampling time ($t_{\mathrm{d}} = 2$ min). Therefore, an augmented state vector is defined as:

$$\tilde{x}(k) = [x_1(k)\dots x_{23}(k) \; u_1(k-1)\dots u_5(k-1)]^T$$

and the system matrices A, B, B_{d}, C, C_{c} and D_{d} are modified accordingly [9]. To simplify the notation, the model form (12) will continue to be used in the subsequent development. The measured disturbance vector includes the customer withdraw rates at each node and the production rate of plant 10-1 where LMPC is not implemented:

$$d = \Bigg[\sum_{i=1}^{4} F_{i,1} \; \sum_{i=5}^{9} F_{i,1} \; F_{10,1} \; \sum_{i=11}^{12} F_{i,1}$$

$$\sum_{i=13}^{17} F_{i,1} \; \sum_{i=18}^{21} F_{i,1} \; \sum_{i=22}^{23} F_{i,1} \; \sum_{i=25}^{26} F_{i,1}$$

$$\sum_{i=27,28,30} F_{i,1} \Bigg]^T$$

where the $F_{i,1}$ denote gas flow rates for the full-order model derived from Fig. 1 and each term in the vector corresponds to the gas flow rate at a node of the

Table 1
Node reduction of the full-order model to generate the plant and controller models

Node	Full model R^{43}	Plant model R^{32}	Control model R^{23}	Node	Full model R^{43}	Plant model R^{32}	Control model R^{23}
1	P_1	P_1	P_{1-4}	21	P_{21}		
2	P_2	$P_{2,4}$	P_{5-9}	22	P_{22}		
3	P_3	P_3	P_{10}	23	P_{23}		
4	P_4	$P_{5,6}$	$P_{11,12}$	24	P_{24}		
5	P_5	P_7	P_{13-17}	25	P_{25}		
6	P_6	$P_{8,9}$	P_{18-21}	26	P_{26}		
7	P_7	P_{10}	$P_{22,23}$	27	P_{27}		
8	P_8	P_{11}	P_{24}	28	P_{28}		
9	P_9	P_{12}	$P_{25,26}$	29	P_{29}		
10	P_{10}	P_{13}	P_{27-30}	30	P_{30}		
11	P_{11}	P_{14}			$F_{10,2}$	$F_{10,2}$	$F_{10,2}$
12	P_{12}	P_{15-17}			$F_{10,3}$	$F_{10,3}$	$F_{10,3}$
13	P_{13}	P_{18-21}			$F_{24,1}$	$F_{24,1}$	$F_{24,1}$
14	P_{14}	P_{22}			$F_{24,2}$	$F_{24,2}$	$F_{24,2}$
15	P_{15}	P_{23}			$F_{29,1}$	$F_{29,1}$	$F_{29,1}$
16	P_{16}	P_{24}			η	η	η
17	P_{17}	$P_{25,26}$			e_{f}	e_{f}	e_{f}
18	P_{18}	$P_{27,28}$			η_{f}	η_{f}	η_{f}
19	P_{19}	$P_{29,30}$			Γ_x	Γ_x	Γ_x
20	P_{20}						

controller model derived from Fig. 3. The pressures at nodes 4, 8 and 10 (see Fig. 3) are controlled to setpoints because these pressures largely determine the entire pipeline pressure distribution:

$$y = \begin{bmatrix} P_{11,12} & P_{24} & P_{27-30} \end{bmatrix}^T$$

There also are 14 output constraint variables which include the three controlled outputs defined above. Additional constrained outputs are the let-down station valve position and the plant constraint variables discussed earlier.

To further establish the need for multivariable control, it is useful to obtain the relative gain array (RGA) for the LMPC design model. The RGA can be used to determine if interactions between single-loop controllers will be problematic. The linear model used for this analysis excludes the let-down station control loop since the let-down control valve position is used as an input in the RGA analysis. The outputs are chosen as the pressures defined above ($P_{11,12}$, P_{24}, P_{27-30}) as well as the pressure downstream of the let-down station (P_{18-21}). The inputs are the total production requests at nodes 10, 24 and 29 of the full-order model (see Fig. 1) and the let-down station valve position. The gain matrix is generated using a method specifically designed for integrating systems [6]:

$$K = \begin{bmatrix} 0.0378 & 0.0378 & 0.0378 & 0.5879 \\ 0.0375 & 0.0375 & 0.0375 & 0.5827 \\ 0.0370 & 0.0370 & 0.0370 & -0.2443 \\ 0.0382 & 0.0382 & 0.0382 & -0.2519 \end{bmatrix}$$

The first three columns contain integrating gains (slopes) between the node pressures and the production requests. The last column contains steady-state gains between the node pressures and the valve position.

The relative gain between controlled variable Y_i and manipulated variable U_j is defined as [21]:

$$\lambda_{i,j} = \frac{\left(\partial Y_i / \partial U_j \right)_U}{\left(\partial Y_i / \partial U_j \right)_Y} \tag{14}$$

Because the gain matrix is singular, the RGA cannot be computed. For this system the closed-loop gain ($\partial Y_i / \partial U_j$)$_Y$ is always zero because the pressure at a given node does not change if the other pressures are held constant. The RGA analysis suggests that single-loop controllers designed using these inputs and outputs will be highly interacting. While it has been shown that LMPC can exhibit robustness problem when applied to systems with large RGA values [22], we have not observed any such problems in our simulations. Therefore, LMPC appears to be an appropriate control strategy for this problem.

2.4. Open-loop simulation

The dynamic models are solved in MATLAB using the SIMULINK integration routine ODE15s [2]. Open-loop responses of the full-order model (Fig. 1) and the plant model (Fig. 2) are compared in Fig. 4 for a positive step change of 50 kcfh in the plant 10-1 product request. All pressures are plotted as deviations from the let-down station pressure, which is controlled at a constant setpoint. This test confirms that the dimensionality reduction used to generate the plant model does not significantly affect the dynamic behavior. The full-order model simulation requires about 20 min for an 8-h simulation on a DEC Alpha 433 workstation, while the plant model simulation takes less than 3 min. The "spikes" observed in the full-order model response are indicative of numerical instability caused by ill-conditioning.

Fig. 5 shows the open-loop responses obtained when the plant model, nonlinear controller model and linear controller model are subjected to the following changes:

1. −25 kcfh change in plant 10-1 production request at $t = 1$ h.
2. +25 kcfh change in plant 10-1 production request at $t = 2.5$ h.
3. +50 kcfh change in node 26 customer withdraw at $t = 5$ h.
4. −50 kcfh change in node 26 customer withdraw at $t = 7.5$ h.

The node pressures on the low pressure side converge to constant values close to the initial steady state because the let-down station pressure is controlled at its setpoint. On the high pressure side, the node pressures increase or decrease with constant slopes after some initial dynamics. The three models show similar trends, so the linear controller model appears to adequately capture the important dynamics of this "slightly" nonlinear process.

3. Linear model predictive control strategy

The infinite horizon LMPC formulation proposed by Muske and Rawlings [15] is applied to the oxygen pipeline. Because this formulation provides nominal stability for unstable systems, it is not necessary to prestabilize the pipeline with a conventional controller prior to applying LMPC. Other advantages of the formulation include flexible use of alternative feedback structures to handle measured and unmeasured disturbances, as well as the explicit incorporation of input and output constraints. Below the LMPC strategy is presented with an emphasis on the specific formulation for the pipeline network.

3.1. LMPC regulator

A necessary condition for LMPC to be applicable is that the linear model is stabilizable. It is easy to show that the augmented linear controller model satisfies this condition. A vector of future inputs, $U^N = [u^T(k|k)\ u^T(k+1|k)\ \ldots\ u^T(k+N\text{-}1|k)]^T$, is calculated by solving the following infinite horizon open-loop optimization problem:

$$\min_{U^N}\ \phi_k = \sum_{j=0}^{\infty}\Big\{[y(k+j|k) - y_s]^T Q[y(k+j|k) - y_s]$$
$$+ [u(k+j|k) - u_s]^T R[u(k+j|k) - u_s]$$
$$+ \Delta u(k+j|k)^T S \Delta u(k+j|k)\Big\} \tag{15}$$

where the double indexed variables $y(k+j|k)$ and $u(k+j|k)$ represent predictions of the output and input variables, respectively, at time $k+j$ based on information at time k; $\Delta u(k+j|k) = u(k+j|k)/u(k+j-1|k)$; y_s and u_s are output and input targets, respectively; Q and S are positive semidefinite penalty matrices; and R is a positive definite penalty matrix. Note that the prediction horizon is infinite, while a finite control horizon (N) is used to yield a finite number of decision variables. Manipulated inputs beyond the control horizon are set equal to their target values:

$$u(k+j|k) = u_s, \quad \forall\ j \geqslant N$$

The infinite horizon problem in (15) can be reformulated as a finite horizon problem [15]:

$$\min_{U^N}\ \phi_k = [x(k+N|k) - x_s]^T \bar{Q}[x(k+N|k) - x_s]$$
$$+ \Delta u(k+N|k)^T S \Delta u(k+N|k)$$
$$+ \sum_{j=0}^{N-1}\Big\{[x(k+j|k) - x_s]^T C^T Q C[x(k+j|k) - x_s]$$
$$+ [u(k+j|k) - u_s]^T R[u(k+j|k) - u_s]$$
$$+ \Delta u(k+j|k)^T S \Delta u(k+j|k)\Big\} \tag{16}$$

where x_s is the target vector for the state variables, and $\bar{Q}$ is the terminal penalty matrix that is computed by solving the appropriate Lyapunov equation [15].

The linearized pipeline model has one eigenvalue on the unit disk. For such unstable systems, the matrix A is partitioned into stable and unstable parts. This is necessary because the unstable modes must be driven to
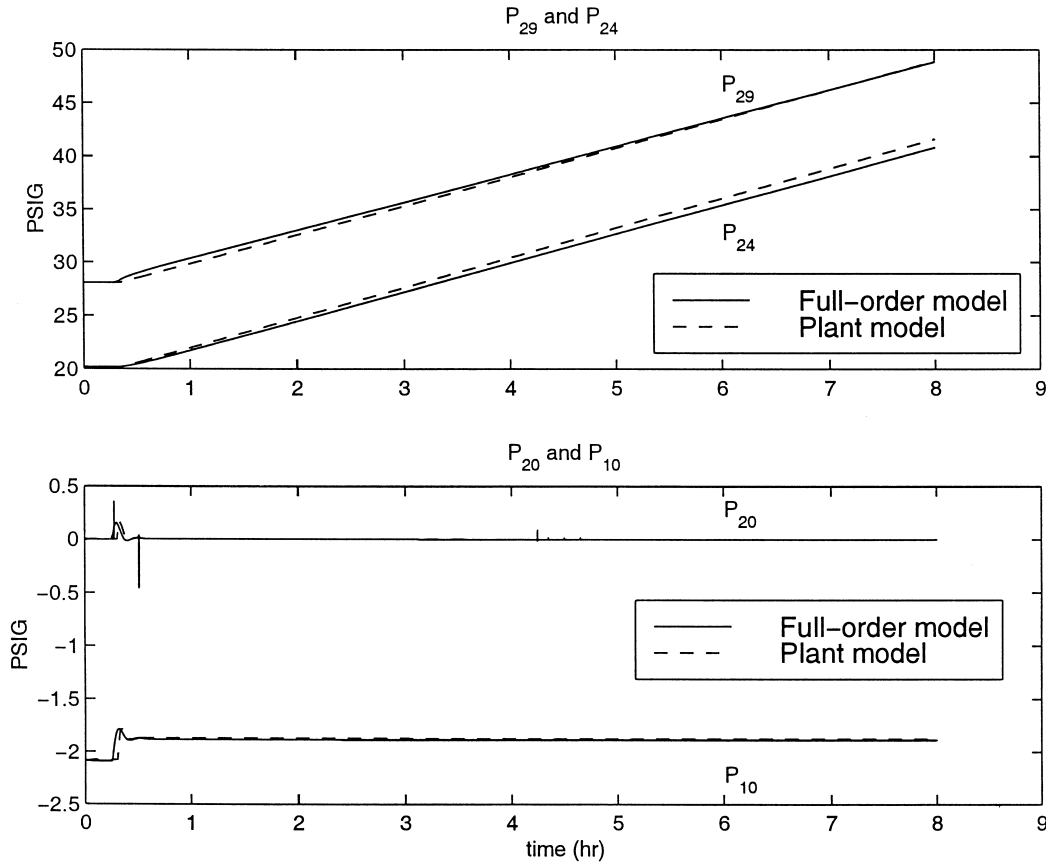

Fig. 4. Open-loop simulation: full-order model and plant model.

their targets by the end of the control horizon so the infinite horizon objective function has a finite value. Partitioning is performed by finding the Jordan form of A [15]:

$$A = VJV^{-1} = \begin{bmatrix} V_u & V_s \end{bmatrix} \begin{bmatrix} J_u & 0 \\ 0 & J_s \end{bmatrix} \begin{bmatrix} \tilde{V}_u \\ \tilde{V}_s \end{bmatrix} \qquad (17)$$

where the diagonal matrices J_u and J_s contain the unstable and stable eigenvalues, respectively, and V_u and V_s are comprised of the corresponding eigenvectors. The state vector is transformed into decoupled unstable (z^u) and stable (z^s) modes as follows:

$$\begin{bmatrix} z^u \\ z^s \end{bmatrix} = \begin{bmatrix} \tilde{V}_u \\ \tilde{V}_s \end{bmatrix} x \qquad (18)$$

The following terminal equality constraint is appended to the optimization problem:

$$z^u(k+N|k) = \tilde{V}_u x_s \qquad (19)$$

The terminal penalty matrix $\bar{Q}$ is computed by solving the Lyapunov equation using only the stable modes [15]:

$$\bar{Q} = \tilde{V}_s^T \Sigma \tilde{V}_s \qquad (20)$$

$$\Sigma = V_s^T C^T Q C V_s + J_s^T \Sigma J_s \qquad (21)$$

With some algebraic manipulation, the optimization problem (16) can be formulated as a quadratic program (QP) for u^N:

$$\min_{U^N} \phi_k = \left(u^N\right)^T H u^N + 2\left(u^N\right)^T [Gx(k) - Fu(k-1)] \qquad (22)$$

The form of the matrices H, G and F can be found in [15]. It is possible to include measured disturbances in the state predictions with minor modification of the QP problem. Because customer withdraw rates cannot be forecasted accurately, we utilize an alternative feedforward control strategy in which the measured disturbances are used to shift the target values [15]. This is discussed below. The following input and output constraints also are considered:

$$u_{min} \leqslant u(k+j|k) \leqslant u_{max} \quad j = 1 \ldots N$$

$$y_{min} \leqslant y_c(k+j|k) \leqslant y_{max} \quad j = 1 \ldots \infty \qquad (23)$$
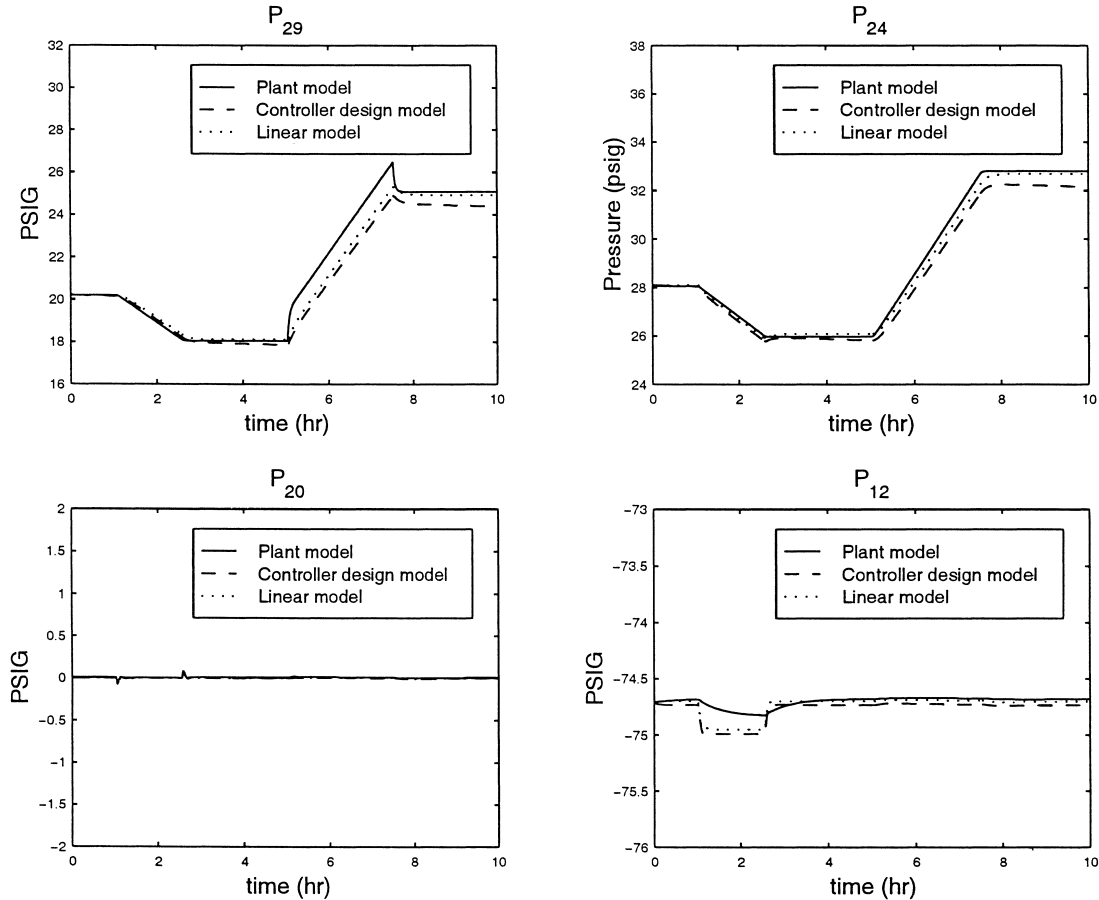

Fig. 5. Open-loop simulation: plant model, controller model and LMPC design model.

Note that the output constraints are to be enforced over the infinite prediction horizon. In some situations, it is necessary to relax the output constraints to achieve feasibility of the QP. The feasibility issue is discussed later in this section.

3.2. Disturbance estimation and steady-state target calculation

The output disturbance model is the most common paradigm for estimating unknown disturbances in LMPC applications. Offset-free tracking performance can be achieved only if there are sufficient degrees of freedom [15]; that is, the number of unconstrained inputs is greater than or equal to the number of outputs. When choosing a feedback structure for the gas pipeline system, the following characteristics need to be considered: (i) there are only six inputs; (ii) 14 outputs must be maintained within constraints, but only three outputs need to be controlled to setpoints; (iii) all the state variables are measurable because they are node pressures, flow rates and controller signals; (iv) the customer withdraw rates are measurable; and (v) the pair (C,A) of the LMPC design model is not observable. A custom disturbance modeling approach is developed to fully exploit these system characteristics.

Instead of a more conventional output or input disturbance model, we take advantage of the fact that all the state variables are measurable and propose a state disturbance model. The difference between the estimated and measured state vectors is assumed to be attributable to a constant step disturbance vector ζ. Therefore, the augmented process model takes the following form:

$$x(k+1) = Ax(k) + Bu(k) + B_\mathrm{d}d(k) + \zeta(k) \tag{24}$$

$$\zeta(k+1) = \zeta(k) \tag{25}$$

Estimates of the disturbance vector are generated using the deadbeat observer:

$$\hat{\zeta}(k-1|k) = x(k) - Ax(k-1) - Bu(k-1)$$
$$- B_\mathrm{d}d(k-1) \tag{26}$$

$$\zeta(k|k) = \hat{\zeta}(k-1|k) \tag{27}$$

Once the disturbance estimates are available, the new steady-state targets for the state and input variables are determined by solving the following QP problem [15]:

$$\min_{x_\mathrm{s}(k),u_\mathrm{s}(k)} [u_\mathrm{s}(k) - u_\mathrm{ref}]^T R_\mathrm{s}[u_\mathrm{s}(k) - u_\mathrm{ref}] \tag{28}$$

subject to:

$$\begin{bmatrix} I - A & -B \\ C & 0 \end{bmatrix} \begin{bmatrix} x_\mathrm{s}(k) \\ u_\mathrm{s}(k) \end{bmatrix} = \begin{bmatrix} B_\mathrm{d}d(k) + \hat{\zeta}(k|k) \\ y_\mathrm{ref} \end{bmatrix}$$
$$u_\mathrm{min} \leqslant u_\mathrm{s}(k) \leqslant u_\mathrm{max}$$

where R_s is a positive definite weighting matrix, and y_ref and u_ref are output and input setpoints, respectively. For the pipeline system, this problem can become infeasible when the number of active input constraints exceeds three. In this case, an alternative QP problem is solved which minimizes the difference between the outputs and their setpoints:

$$\min_{x_\mathrm{s}(k),u_\mathrm{s}(k)} [y_\mathrm{ref} - Cx_\mathrm{s}(k)]^T Q_\mathrm{s}[y_\mathrm{ref} - Cx_\mathrm{s}(k)] \tag{29}$$

subject to:

$$\begin{bmatrix} I - A & -B \end{bmatrix} \begin{bmatrix} x_\mathrm{s}(k) \\ u_\mathrm{s}(k) \end{bmatrix} = \begin{bmatrix} B_\mathrm{d}d(k) + \hat{\zeta}(k|k) \end{bmatrix}$$

$$u_\mathrm{min} \leqslant u_\mathrm{s}(k) \leqslant u_\mathrm{max}$$

where Q_s is a positive definite weighting matrix. A necessary condition for the target calculation to be feasible is that the measured disturbances satisfy:

$$\sum_{i=1}^{10} d_i(k) \leqslant \sum_{j=1}^{5} u_{\mathrm{max}_j} \tag{30}$$

which mathematically states the obvious condition that the system does not have a steady-state solution if the combined customer withdraws exceeds the total capacity of the cryogenic plants.

3.3. Output constraint handling

As discussed previously, output constraints of the following form are considered:

$$y_\mathrm{min} \leqslant y_\mathrm{c}(k+j|k) \leqslant y_\mathrm{max} \quad j = 1...\infty \tag{31}$$

The output constraints can be reformulated as [17]:

$$\hat{H}x(k+j|k) \leqslant h \quad j = 1...\infty \tag{32}$$

where $\hat{H}$ is a constant matrix and the vector h has all positive elements. A key feature of any LMPC strategy is the method used to relax the output constraints to achieve feasibility of the QP. While other techniques are available [20], only the three output handling methods discussed below are considered in this paper.

Rawlings and Muske [17] propose the relaxation of output constraints during the initial portion of the prediction horizon when an infeasibility is encountered. They show the existence of a finite number k_1 such that the

output constraints are guaranteed to be feasible for all $k > k_1$. For unstable systems, k_1 can be computed as [17]:

$$k_1 = N + \max \left\{ \ln \left(\frac{h_{\min}}{\| \hat{H} \| \| V_s \| \| z^s(k + N|k) \|} \right) / \ln(\lambda_{\max}), 1 \right\}$$

(33)

where $\lambda_{\max}$ is the largest eigenvalue of J_s and $h_{\min}$ is the smallest element of vector h. Rawlings and Muske [17] also show the existence of a finite k_2 such that the output constraints are enforced over the rest of the infinite horizon if they are satisfied between k_1 and k_2. This is called the hard constraint handling method. For the pipeline system, the values of k_1 and k_2 calculated from these formulas can be very large (> 1000) because the largest stable eigenvalue (0.995) is very close to unity. This makes the constraint handling method rather difficult to implement.

To address this limitation, we propose an alternative hard constraint handling method. When an infeasibility occurs, the output constraints are removed at the first time step in the horizon and the QP is resolved. If the QP remains infeasible, then the output constraints at the second time step also are removed and the QP is resolved. This procedure is continued until the QP problem is feasible. The advantage of this approach is that the output constraints are relaxed the minimum number of times required to obtain feasibility. A shortcoming is that a potentially large number of QP problems must be solved at a single time step. For the pipeline system, we have found that the constraints must be removed only at the first one or two steps in the horizon. The problem of large k_2 values is circumvented by enforcing the output constraints only up to the control horizon N. Clearly, this approach does not guarantee that the constraints are satisfied over the entire horizon.

Zheng and Morari [24] propose an output constraint handling method in which slack variables are introduced to soften the output constraints. The slack variables are penalized by a positive definite weighting matrix P_s in the objective function. The following LMPC problem is obtained:

$$\min_{U^N, s(k)} \phi_k = [x(k + N|k) - x_s]^T \bar{Q}[x(k + N|k) - x_s]$$

$$+ \Delta u(k + N|k)^T S \Delta u(k + N|k)$$

$$+ \sum_{j=0}^{N-1} \left\{ [x(k + j|k) - x_s]^T C^T Q C[x(k + j|k) - x_s] \right.$$

$$+ [u(k + j|k) - u_s]^T R[u(k + j|k) - u_s]$$

$$+ \left. \Delta u(k + j|k)^T S \Delta u(k + j|k) + s(k)^T P_s s(k) \right\}$$

$$y_{\min} - s(k) \leqslant y_c(k + j|k) \leqslant y_{\max} + s(k) \quad j = 1, ..., N \quad (34)$$

where $s(k)$ is a vector of slack variables. Again the output constraints are only enforced over the control horizon N. To formulate the QP, the output constraints are written as inequality constraints in terms of u^N and $s(k)$:

$$\begin{bmatrix} D \\ -D \end{bmatrix} \begin{bmatrix} u^N \\ s(k) \end{bmatrix} \leqslant \begin{bmatrix} d_1 \\ d_2 \end{bmatrix}$$

(35)

The formulation of D, d_1 and d_2 can be found in [15].

4. Simulation results and discussion

We now apply the LMPC controller to the simulated oxygen pipeline network. The reduced-order nonlinear plant model (see Fig. 2) is used to represent the pipeline network. The control horizon is $N = 15$, and the quadratic weighting matrices in the objective function are chosen as: $Q = I_{3\times3}$, $R = 0.1I_{6\times6}$, $S = 100I_{6\times6}$. When the soft output constraint handling method is used, the penalty matrix P_s on the slack variables is chosen as $50I_{14\times14}$. These tuning parameters were determined by trial and error. Except for the let-down station valve position, the input and output constraints in deviations from the nominal steady states are:

$$\begin{bmatrix} -200 & \text{kcfh} \\ -150 & \text{kcfh} \\ -200 & \text{kcfh} \\ -200 & \text{kcfh} \\ -210 & \text{kcfh} \\ -14.9 & \text{psig} \end{bmatrix} \leqslant u(k) \leqslant \begin{bmatrix} 150 & \text{kcfh} \\ 150 & \text{kcfh} \\ 100 & \text{kcfh} \\ 100 & \text{kcfh} \\ 190 & \text{kcfh} \\ 25.1 & \text{psig} \end{bmatrix}$$

$$\begin{bmatrix} -5.2 & \text{psig} \\ -23 & \text{psig} \\ -35.1 & \text{psig} \\ 0\% \\ \Gamma_{\min} \end{bmatrix} \leqslant y_c(k) \leqslant \begin{bmatrix} 29.8 & \text{psig} \\ 17 & \text{psig} \\ 24.9 & \text{psig} \\ 90\% \\ \Gamma_{\max} \end{bmatrix}$$

The limits $\Gamma_{\max}$ and $\Gamma_{\min}$ for the plant constraint variables are not reported for proprietary reasons. However, it is important to emphasize that none of these constraints are active during any of the following simulation tests. All simulations are performed in MATLAB on a DEC Alpha 433 workstation. A typical closed-loop simulation of 8 hours requires approximately 5 min of CPU time.

Fig. 6 shows stabilization of the pipeline network at the nominal steady state. The figure includes the first four constrained outputs (including the three pressures controlled to setpoints) and the six manipulated inputs. The dotted lines represent the setpoints for the outputs and the actual flow rates corresponding to the first five

inputs. For the last input, the dotted line represents the actual let-down station pressure. Because the controller design model is a reduced-order linear approximation of the plant model, there is plant/model mismatch even at steady state. This test shows that the LMPC controller is capable of handling the mismatch as the pressures are maintained within one psig of the desired steady-state values.

Fig. 7 shows the closed-loop response for $+10$ psig setpoint changes in the node 24 and 29 pressures (see Fig. 1) at $t = 3$ h. Setpoint changes of the same magnitude are introduced since these two pressures should have a relatively constant pressure difference. This test simulates a desired pressure build-up on the high pressure side of the network to take advantage of low utility costs at off-peak hours. The initial transient is due to plant/model mismatch as discussed above. The new setpoints are achieved about 2 h after the requests are issued, and the pressure at node 12 is kept very close to its setpoint. The let-down valve is closed about 10%
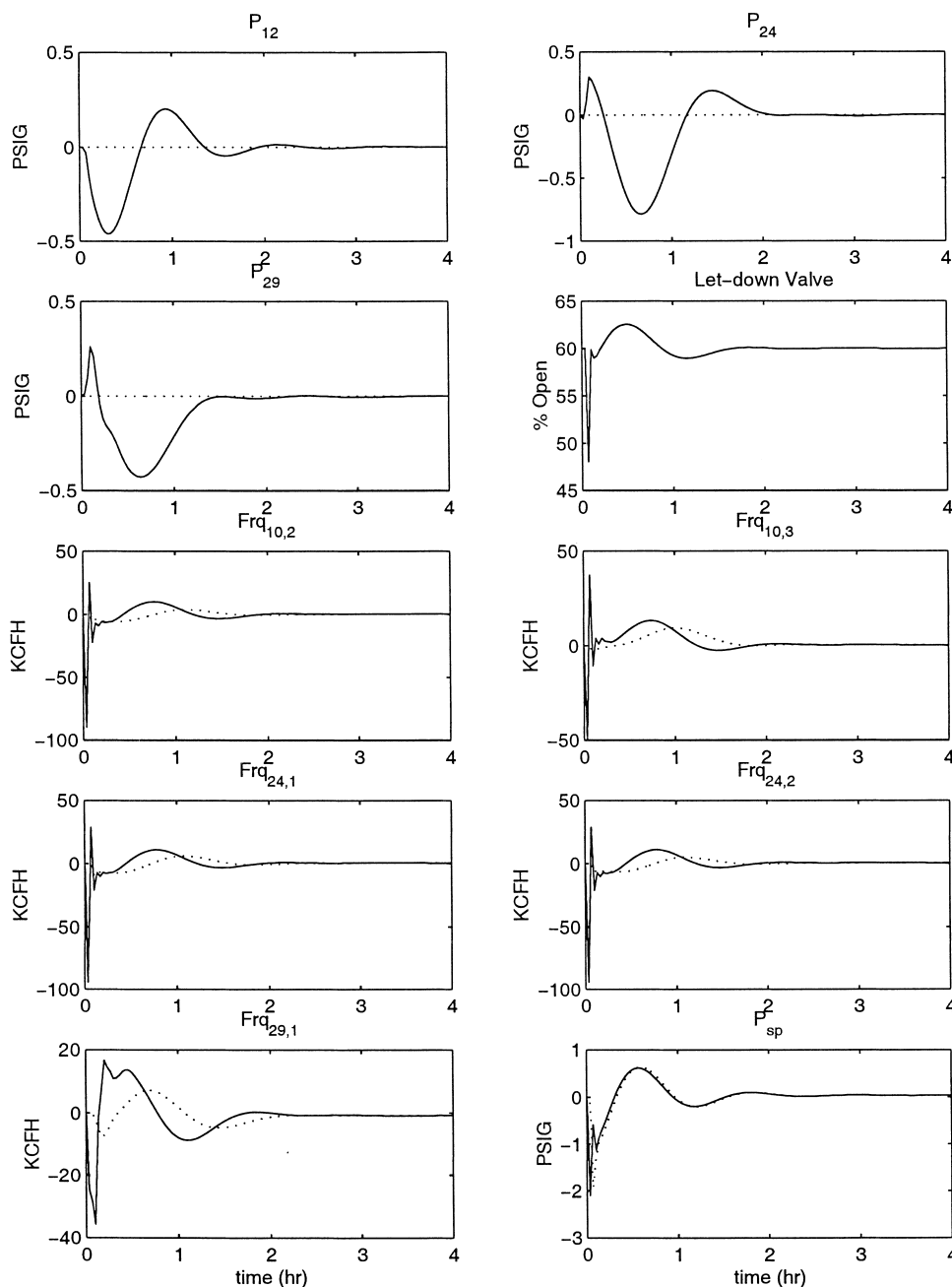

Fig. 6. Nominal stabilization.

because the pressure drop across the valve is increased. For the first five inputs, the production requests (solid lines) increase rapidly when the setpoint changes are implemented. The production requests for two plants reach their upper limits for a brief period of time. The actual production rates follow the flow requests according to the first-order-plus-deadtime models used to model the closed-loop cryogenic plant dynamics.

The results obtained for two measured customer withdraw rate changes are shown in Fig. 8. At $t=3$ h

the customer withdraw rate at node 24 is increased by 100 kcfh, then at $t=8$ h the customer withdraw rate at node 1 is increased by 150 kcfh. This test models a combination of smaller customer withdraw rate changes near these nodes. Both disturbances are rejected with only small deviations of the outputs from their setpoints. The same test has been performed with the withdraw rates considered as unmeasured disturbances. Since a dead-beat observer is used to generate the disturbance estimates, and the entire state vector is measured, the controller
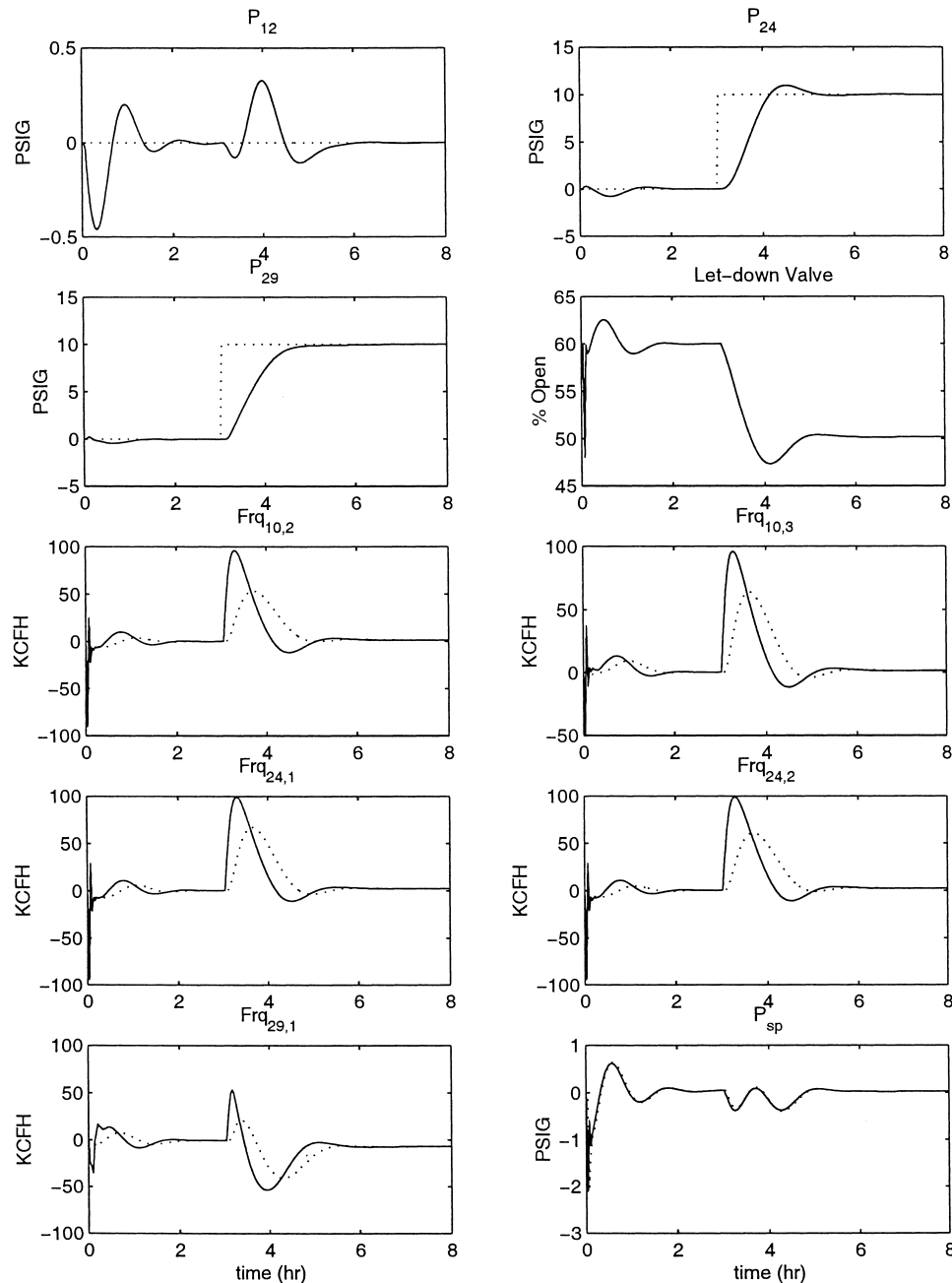

Fig. 7. Setpoint changes.

responds very quickly to the demand changes. As a result, the closed-loop response is virtually identical to Fig. 8 and is not shown here.

First-order-plus-dead-time (FOPDT) models obtained from plant tests are used to model the dynamics of the LMPC controlled cryogenic plants. In practice, the actual closed-loop plant behavior will deviate from the FOPDT model predictions. To examine the ability of the LMPC controller to handle this uncertainty, the time constant of each FOPDT model in the simulated plant is

increased by 15 min (60–100% increase) while the controller design model is unchanged. The closed-loop response for the same disturbance sequence as in Fig. 8 is shown in Fig. 9. The controller rejects the measured disturbances quite effectively despite the modeling error. Although slightly larger production request changes are observed, the output responses are very similar to those obtained for a perfect model (Fig. 8).

The complete shut-down of plant 10-1 represents a very large measured disturbance that is simulated to test
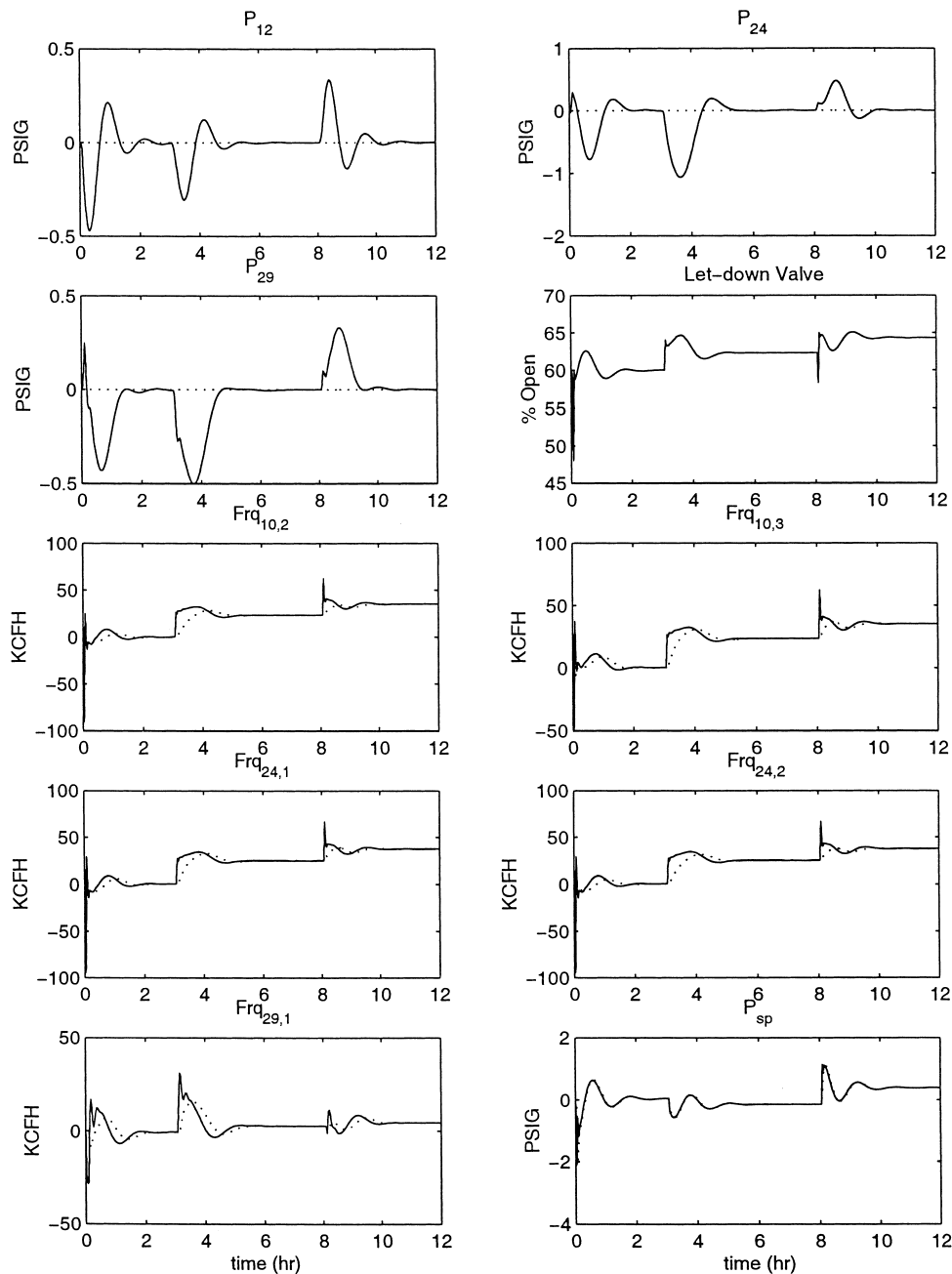

Fig. 8. Disturbance rejection for known changes in customer withdraw.

the constraint handling abilities of the LMPC controller. The upper constraint for the let-down valve position is reduced to 85% to allow output constraint violations to be examined more easily. Fig. 10 shows the results obtained with the soft output constraint handling method [24]. When the plant shut-down occurs at $t = 3$ h, the pipeline pressures on the low pressure side drop rapidly. Production requests are driven to their upper limits to compensate for the pressure loss. Note that the node 29 pressure exhibits a large overshoot

immediately after the initial pressure drop. This can be explained by noting that node 29 is on the high pressure side of the let-down valve while plant 10-1 is on the low pressure side. The plant 29-1 production rate responds quickly to the disturbance and causes the node pressures on the high pressure side to increase. Two different slack variable penalty matrices have been evaluated. When $P_s = 50I$, the valve position (solid line) barely violates its upper limit. When $P_s = I$, the valve position (dashed line) exhibits a significant violation of the upper constraint.
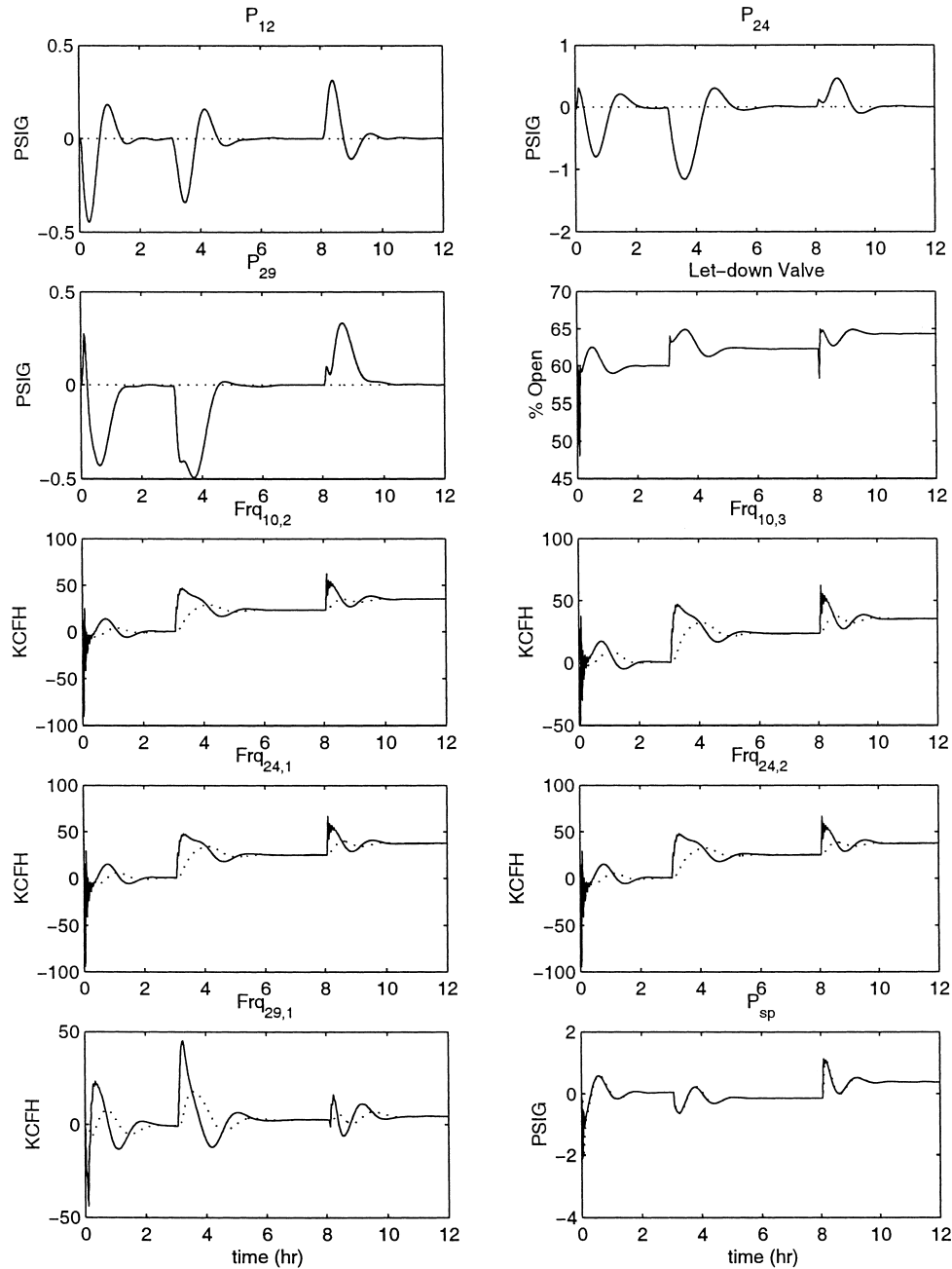

Fig. 9. Disturbance rejection for known changes in customer withdraws with modeling errors in the cryogenic plant responses.

The responses of the other variables are nearly identical. Clearly the tuning of P_s plays a critical role in the constraint handling behavior of the LMPC controller.

The hard output constraint method is not evaluated because the large k_1 values calculated from (33) effectively eliminates the output constraints over the entire horizon. In Fig. 11, the alternative hard output constraint method described earlier is evaluated for the same disturbance and output constraints as in Fig. 10. The output and input responses are very similar to those obtained with the soft constraint handling method (Fig. 10). The QP remains feasible except at a few time steps where the upper valve position constraint is violated. At those time steps, feasibility is established by removing the output constraints only at the first time step and enforcing the constraints over the rest of the horizon $j \epsilon [k+1, N]$. This procedure allows the valve position constraint to be violated only very slightly. Because this output constraint handling method may require the solution of a large number of QP problems
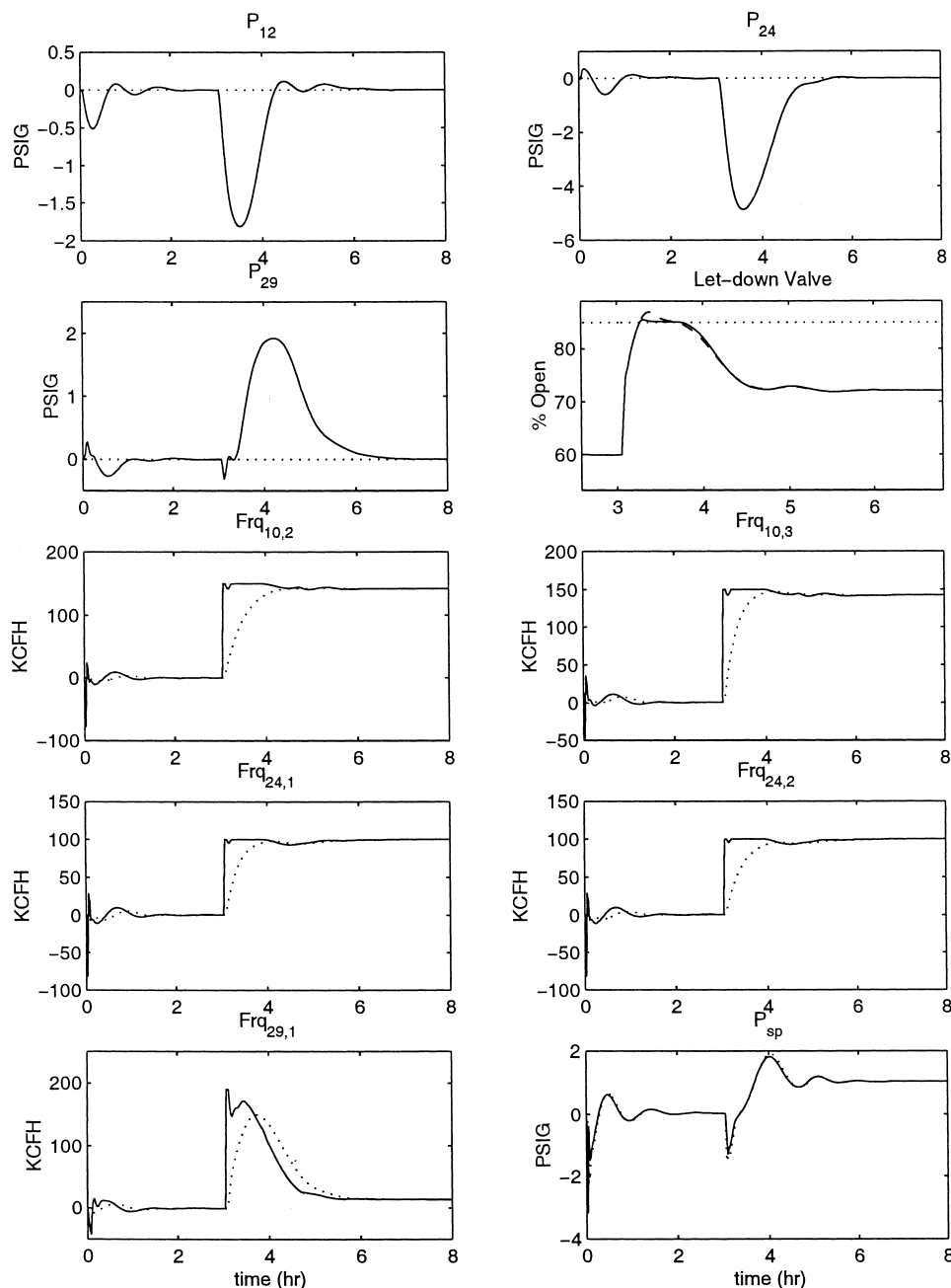

Fig. 10. Disturbance rejection for known plant shutdown using the soft constraint handling method: $P_s = 50I$ (solid line), $P_s = I$ (dashed line).
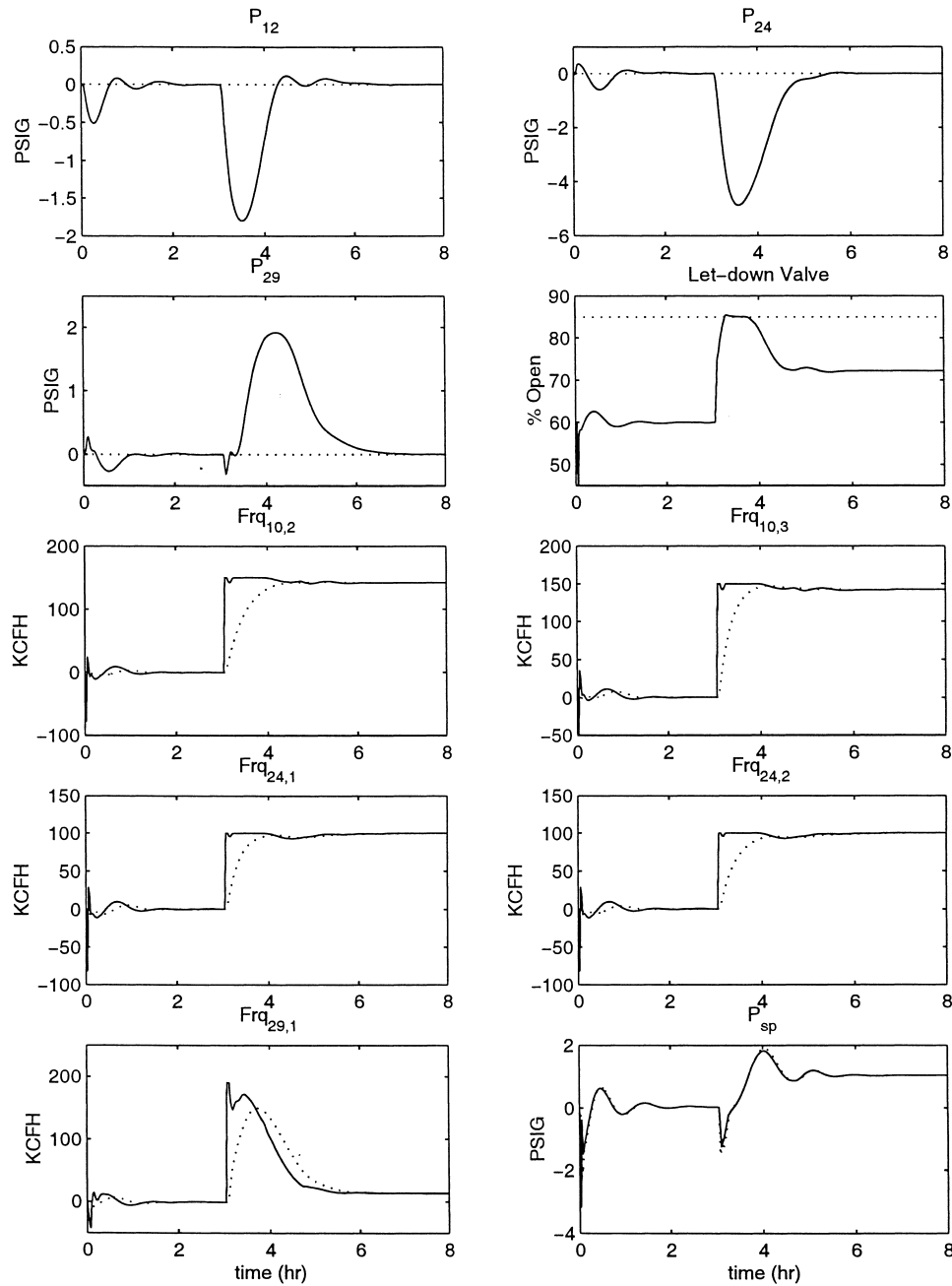
Fig. 11. Disturbance rejection for known plant shutdown using the alternative hard constraint handling method.

when an infeasibility is encountered, careful tuning of the soft output constraint handling method appears to be preferred for this problem.

5. Summary and conclusions

Effective control of large-scale gas pipeline networks is required to ensure safe and profitable operation. While pipelines are critical in the air separation and natural gas industries, the application of advanced con-

trol to such systems is not currently practiced. We have developed and evaluated a linear model predictive control (LMPC) strategy for a simulated industrial-scale oxygen pipeline network. A first-principles nonlinear model for the node pressures is derived from mass balances and the Virial equation of state. The LMPC design is based on a linearized model derived from a reduced-order nonlinear pipeline model. Both measured and unmeasured disturbances are systematically incorporated in the LMPC target calculations. The LMPC controller provides excellent closed-loop performance

for a wide variety of setpoint changes and disturbances. Three output constraint handling techniques to resolve infeasibilities in the LMPC quadratic program have been examined. We believe that the proposed LMPC strategy can significantly improve the operability of large-scale gas pipeline networks and can enable gas suppliers to take full advantage of the deregulation of the utility industry.

Appendix A. Nomenclature

B_i	second Virial coefficient at node i (ft^3)
C_v	valve characteristic constant
d_p	pipe diameter (in)
E_f	pipe efficiency factor
e_f	pressure control loop filtered error
$F_{i,1}$	withdraw rate (kcfh) at node i, $i = 1, 4, 6, 9, 11, 12, 14, 16, 17, 19, 22, 25, 26, 28, 30$
$F_{10,j}$	production rate (kcfh) of plant 10-j, $j = 1, 2, 3$
$F_{24,j}$	production rate (kcfh) of plant 24-j, $j = 1, 2$
$F_{29,j}$	production rate (kcfh) of plant 29-1
f_r	friction factor
$Frq_{10,j}$	production setpoint (kcfh) of plant 10-j, $j = 2, 3$
$Frq_{24,j}$	production setpoint (kcfh) of plant 24-j, $j = 1, 2$
$Frq_{29,j}$	production setpoint (kcfh) of plant 29-1
K_c	let down station controller gain (%/psig)
L	pipe length (mile)
l	percent valve opening
N_i	molar holdup (lb-mol) at node i
P_i	pressure (psig) at node i
P_{sp}	setpoint (psig) for let-down pressure controller
R	gas constant (psia-ft^3/lbmol-R)
S_g	oxygen specific gravity
T	pipeline temperature (R)
t_d	dead time of closed-loop plants (min)
V_i	node volume i (ft^3)
Z_m	mean compressibility

Greek Letters

Γ	plant constraint vector
Γ_x	subset of plant constraint variables used as state variables
η	pressure control loop accumulated error
η_f	filtered accumulated error

ρ_{sc}	molar density (lbmol/ft^3) of O_2 at 1 atm and 60°F
$\tau_{10,j}$	time constant of closed-loop cryogenic plant 10-j, $j = 2, 3$
$\tau_{24,j}$	time constant of closed-loop cryogenic plant 24-j, $j = 1, 2$
$\tau_{29,1}$	time constant of closed-loop cryogenic plant 29-1
τ_f	PI controller error filter time constant
τ_I	PI controller integral time
θ	pipe leg parameters

Superscripts

ss	steady-state value

Appendix B. Full-order model

$$\dot{P}_1(t) = \rho_{sc}f_2(P_1)\big[f_1(P_1, P_2) + F_{1,1}\big]$$

$$\dot{P}_2(t) = \rho_{sc}f_2(P_2)[f_1(P_2, P_1) + f_1(P_2, P_3) + f_1(P_2, P_4)]$$

$$\dot{P}_3(t) = \rho_{sc}f_2(P_3)[f_1(P_3, P_2) + f_1(P_3, P_5)]$$

$$\dot{P}_4(t) = \rho_{sc}f_2(P_4)\big[f_1(P_4, P_2) + F_{4,1}\big]$$

$$\dot{P}_5(t) = \rho_{sc}f_2(P_5)[f_1(P_5, P_3) + f_1(P_5, P_6) + f_1(P_5, P_7)]$$

$$\dot{P}_6(t) = \rho_{sc}f_2(P_6)\big[f_1(P_6, P_5) + F_{6,1}\big]$$

$$\dot{P}_7(t) = \rho_{sc}f_2(P_7)[f_1(P_7, P_5) + f_1(P_7, P_8)]$$

$$\dot{P}_8(t) = \rho_{sc}f_2(P_8)[f_1(P_8, P_7) + f_1(P_8, P_9) + f_1(P_8, P_{10})]$$

$$\dot{P}_9(t) = \rho_{sc}f_2(P_9)\big[f_1(P_9, P_8) + F_{9,1}\big]$$

$$\dot{P}_{10}(t) = \rho_{sc}f_2(P_{10})\big[f_1(P_{10}, P_8) + f_1(P_{10}, P_{11}) + f_1(P_{10}, P_{13}) + F_{10,1} + F_{10,2} + F_{10,3}\big]$$

$$\dot{P}_{11}(t) = \rho_{sc}f_2(P_{11})\big[f_1(P_{11}, P_{10}) + f_1(P_{11}, P_{12}) + F_{11,1}\big]$$

$$\dot{P}_{12}(t) = \rho_{sc}f_2(P_{12})\big[f_1(P_{12}, P_{11}) + F_{12,1}\big]$$

$$\dot{P}_{13}(t) = \rho_{sc}f_2(P_{13})\big[f_1(P_{13}, P_{10}) + f_1(P_{13}, P_{14}) + f_1(P_{13}, P_{15})\big]$$

$$\dot{P}_{14}(t) = \rho_{sc}f_2(P_{14})\big[f_1(P_{14}, P_{13}) + F_{14,1}\big]$$

$$\dot{P}_{15}(t) = \rho_{sc}f_2(P_{15})[f_1(P_{15}, P_{13}) + f_1(P_{15}, P_{16})$$
$$+ f_1(P_{15}, P_{17}) + f_1(P_{15}, P_{18})]$$

$$\dot{P}_{16}(t) = \rho_{sc}f_2(P_{16})[f_1(P_{16}, P_{15}) + F_{16,1}]$$

$$\dot{P}_{17}(t) = \rho_{sc}f_2(P_{17})[f_1(P_{17}, P_{15}) + F_{17,1}]$$

$$\dot{P}_{18}(t) = \rho_{sc}f_2(P_{18})[f_1(P_{18}, P_{15}) + f_1(P_{18}, P_{19})$$
$$+ f_1(P_{18}, P_{20})]$$

$$\dot{P}_{19}(t) = \rho_{sc}f_2(P_{19})[f_1(P_{19}, P_{18}) + F_{19,1}]$$

$$\dot{P}_{20}(t) = \rho_{sc}f_2(P_{20})[f_1(P_{20}, P_{18}) + f_1(P_{20}, P_{21})$$
$$+ f_1(P_{20}, P_{22}, l)]$$

$$\dot{P}_{21}(t) = \rho_{sc}f_2(P_{21})[f_1(P_{21}, P_{20}) + F_{21,1}]$$

$$\dot{P}_{22}(t) = \rho_{sc}f_2(P_{22})[f_1(P_{22}, P_{23}) + f_1(P_{22}, P_{20}, l)]$$

$$\dot{P}_{23}(t) = \rho_{sc}f_2(P_{23})[f_1(P_{23}, P_{22}) + f_1(P_{23}, P_{24})$$
$$+ f_1(P_{23}, P_{25})]$$

$$\dot{P}_{24}(t) = \rho_{sc}f_2(P_{24})[f_1(P_{24}, P_{23}) + F_{24,1} + F_{24,2}]$$

$$\dot{P}_{25}(t) = \rho_{sc}f_2(P_{25})[f_1(P_{25}, P_{23}) + f_1(P_{25}, P_{26})$$
$$+ f_1(P_{25}, P_{27}) + F_{25,1}]$$

$$\dot{P}_{26}(t) = \rho_{sc}f_2(P_{26})[f_1(P_{26}, P_{25}) + F_{26,1}]$$

$$\dot{P}_{27}(t) = \rho_{sc}f_2(P_{27})[f_1(P_{27}, P_{25}) + f_1(P_{27}, P_{28})$$
$$+ f_1(P_{27}, P_{29})]$$

$$\dot{P}_{28}(t) = \rho_{sc}f_2(P_{28})[f_1(P_{28}, P_{27}) + F_{28,1}]$$

$$\dot{P}_{29}(t) = \rho_{sc}f_2(P_{29})[f_1(P_{29}, P_{27}) + f_1(P_{29}, P_{30}) + F_{29,1}]$$

$$\dot{P}_{30}(t) = \rho_{sc}f_2(P_{30})[f_1(P_{30}, P_{29}) + F_{30,1}]$$

$$\dot{F}_{10,2}(t) = \frac{1}{\tau_{10,2}}[Frq_{10,2}(t - t_d) - F_{10,2}(t)]$$

$$\dot{F}_{10,3}(t) = \frac{1}{\tau_{10,3}}[Frq_{10,3}(t - t_d) - F_{10,3}(t)]$$

$$\dot{F}_{24,1}(t) = \frac{1}{\tau_{24,1}}[Frq_{24,1}(t - t_d) - F_{24,1}(t)]$$

$$\dot{F}_{24,2}(t) = \frac{1}{\tau_{24,2}}[Frq_{24,2}(t - t_d) - F_{24,2}(t)]$$

$$\dot{F}_{29,1}(t) = \frac{1}{\tau_{29,1}}[Frq_{29,1}(t - t_d) - F_{29,1}(t)]$$

$$l = l_{ss} + K_c e_f + \frac{K_c}{\tau_I}\eta_f$$

$$\dot{\eta}(t) = P_{sp} - P_{20}$$

$$\dot{e}_f(t) = \frac{1}{\tau_f}(P_{sp} - P_{20} - e_f)$$

$$\dot{\eta}_f = \frac{1}{\tau_f}(\eta - \eta_f)$$

References

[1] Flow of Fluids through Valves, Fittings and Pipe, Crane, Co, Joliet, IL, 1988.
[2] SIMULINK: Dynamic System Simulation for MATLAB, The Mathworks Inc, Natick, MA, 1997.
[3] Large-scale pipeline control relies on advanced systems. Pipeline and Gas Journal, 226:58-59, 1999.
[4] WinTran. Gregg Engineering, Houston, TX (http://www.gregg-engineering.com).
[5] PIPESYS. AEA Technology, Calgary, Alberta (http://www.hy-protech.com).
[6] Y. Akrun, J. Downs, A general method to calculate input-output gains in the relative gain array for integrating process, Computers Che. Engng. 14 (1101–1110) 1990.
[7] E.H. Batey, H.R. Courts, K.W. Hannah, Dynamic approach to gas-pipeline analysis, Oil Gas J. 59 (1961) 65–78.
[8] R. Bomar, Case study: automating a pipeline's control system, Oil Gas J. 96 (1998) 50–55.
[9] G.F. Franklin, J.D. Powell, Digital Control of Dynamic Systems, Addison-Wesley, Reading, MA, 1990.
[10] M.S. Gelormino, N.L. Ricker, Model-predictive control of a combined sewer system, Int. J. Control 59 (1994) 793–816.
[11] J.J. Guy, Computation of unsteady gas flow in pipe networks, in: I. Chem. E. Symp. Ser., 1967, p. 139.
[12] G. Lappus, G. Schmidt, Supervision and control gas transportation and distribution systems, in: 6th IFAC/IFIP Conference on Digital Computer Applications to Process Control, Dusseldorf, Germany, 1980.
[13] D. Marques, M. Morari, On-line optimisation of gas pipelines networks, Automatica 24 (1988) 455–469.
[14] K.R. Muske, J.B. Rawlings, Linear model predictive control of unstable processes, J. Process Control 3 (1993) 85–96.
[15] K.R. Muske, J.B. Rawlings, Model predictive control with linear models, AIChE J. 39 (1993) 262–287.
[16] S.J. Qin, T.A. Badgwell, An overview of industrial model predictive control technology, in: Chemical Process Control-V: Assessment and New Directions for Research, Tahoe City, CA, 1997, pp. 232-256.
[17] J.B. Rawlings, K.R. Muske, The stability of constrained receding horizon control, IEEE Trans. Autom. Control AC-38 (1512-1516) 1993.

[18] K. Sanada, A. Kitagawa, Robust control of a closed-loop pressure control system considering pipeline dynamics, Trans. of the Japan Society of Mechanical Engineers 61 (3559-3566) 1995.

[19] G. Schmidt, A. Wiemann, G. Lappus, Application of simulation techniques to planning, supervision and control of natural-gas distribution networks, in: Simulation, Modelling and Decision in Energy Systems, Montreal, 1978.

[20] J.B. Rawlings, P.O.M Scokaert, Feasability issues in linear model predictive control, AIChE J. 45 (1649-1659) 1999.

[21] D.E. Seborg, T.F. Edgar, D.A. Mellichamp, Process Dynamics and Control, Wiley, New York, NY, 1989.

[22] S. Skogestad, M. Morari, Implications of large RGA elements on control performance, Ind. Eng. Chem. Res. 26 (2323-2330) 1987.

[23] J.M. Smith, H.C. Van Ness, Introduction to Chemical Engineering Thermodynamics, McGraw-Hill, New York, 1975.

[24] A. Zheng, M. Morari, Stability of model predictive control with mixed constraints, IEEE Tran. Automat. Contr. 40 (1818-1823) 1995.